Steven Bunch is a graduate student at the University of Tennessee in Knoxville (UTK) majoring in Electrical Engineering (EE) with a concentration in Analog Electronics. He received his bachelor of science degree at UTK in EE in 2003. In the summer of 2002 he was offered an internship at Oak Ridge National Laboratory to help with programming an accumulator ring dynamics simulation tool for the Spallation Neutron Source (SNS). After finishing his internship he stayed on at the SNS and helped with physics studies of the ring using the tool he built. He continues to work at the SNS programming applications to run the machine. Someday he hopes to pursue his PhD in EE and either become a professor or an entrepreneur.

Jeff Holmes is a Senior Scientist in Accelerator Physics at Oak Ridge National Laboratory. He is a member of the Accelerator Physics Group in the Spallation Neutron Source Project where he specializes in computational beam dynamics. Jeff graduated from Princeton University with a bachelor's degree in electrical engineering and from California Institute of Technology with a PhD in Physics. Following his graduate research in nuclear astrophysics, Jeff joined the staff of Oak Ridge National Laboratory where he worked in the magnetic fusion program as a computational plasma physicist. In 1996 Jeff joined the SNS Project and has since been working in accelerator physics. Aside from physics, Jeff enjoys his family, reading, cinema, exercise, and travel.

EFFECTS AND CORRECTION OF CLOSED ORBIT MAGNET ERRORS IN THE SNS RING

STEVEN C. BUNCH, JEFF HOLMES, PH.D.

ABSTRACT

We consider the effect and correction of three types of orbit errors in SNS: quadrupole displacement errors, dipole displacement errors, and dipole field errors. Using the ORBIT beam dynamics code, we focus on orbit deflection of a standard pencil beam and on beam losses in a high intensity injection simulation. We study the correction of these orbit errors using the proposed system of 88 (44 horizontal and 44 vertical) ring beam position monitors (BPMs) and 52 (24 horizontal and 28 vertical) dipole corrector magnets. Correction is carried out numerically by adjusting the kick strengths of the dipole corrector magnets to minimize the sum of the squares of the BPM signals for the pencil beam. In addition to using the exact BPM signals as input to the correction algorithm, we also consider the effect of random BPM signal errors. For all three types of error and for perturbations of individual magnets, the correction algorithm always chooses the three-bump method to localize the orbit displacement to the region between the magnet and its adjacent correctors. The values of the BPM signals resulting from specified settings of the dipole corrector kick strengths can be used to set up the orbit response matrix, which can then be applied to the correction in the limit that the signals from the separate errors add linearly. When high intensity calculations are carried out to study beam losses, it is seen that the SNS orbit correction system, even with BPM uncertainties, is sufficient to correct losses to less than 10-4 in nearly all cases, even those for which uncorrected losses constitute a large portion of the beam.

INTRODUCTION

The correction of magnet alignment and field errors in high energy particle accelerators is an essential and well-understood subject. Because of the exceedingly high precision required in these machines, the magnet errors must be small and there must be provisions to correct the orbit deviations of the beam particles caused by those errors. Orbit deviations are normally detected by beam position moniters (BPMs), located at various positions in the accelerator, that measure the transverse position of the passing beam. These measured deviations are then corrected through the use of dipole corrector magnets, also located around the accelerator, which kick the beam to straighten the orbit. The accumulator ring of the Spallation Neutron Source (SNS), now under construction at Oak Ridge National Laboratory, will support an extremely intense proton beam, and this paper presents the initial study of orbit errors and their correction in the SNS ring.

The SNS ring will be required to accumulate in excess of 10^{14} protons at 1 GeV during a time span of approximately 1 ms, or about 1000 turns of the 248 m ring. At a pulse rate of 60 Hz, the beam intensity will be in the megawatt range, and unprecedented low loss constraints will be required. At megawatt powers, the fractional beam loss requirements are 10^{-4} for uncontrolled losses and 10^{-3} for total losses including the collimation system. Because magnet errors can contribute significantly to degradation of beam quality and to beam loss, it is essential to study their effect and to provide for their correction. In response to this need, the authors have developed a comprehensive family of computational models for magnet field and alignment errors. In this paper, we present our initial applications of these models by examining some of the most serious errors, namely dipole and quadrupole errors that deflect the closed orbit. In particular, we examine quadrupole and dipole displacement errors as well as dipole field errors.

The SNS ring is 248 m long and consists of four superperiods. Each period contains a 90˚ achromatic arc of four FODO

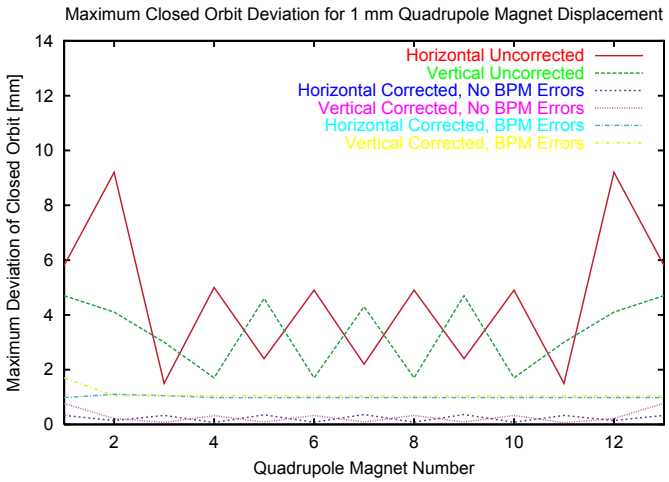

Figure 1. Maximum deviation of pencil beam orbit for 1 mm magnet displacement.

cells with nine quadrupoles and eight dipole magnets, as well as a straight section containing two doublet cells and ample drift spaces for insertions. The basic structure of the SNS Ring lattice is shown in Table 1. Each FODO cell is seen to be eight meters in length, so that the arc is 32 meters long; adding to this the 30 meter length of the straight section, we obtain 62 meters for each superperiod and 248 meters for the ring. This basic structure is supplemented by small dipole, quadrupole, sextupole, and octupole corrector magnets, by various diagnostic apparatus, and by the insertion elements. The insertions in the four straight sections include the injection chicane, collimation, extraction, and RF, respectively. The details of these supplemental elements are too many to be discussed here, but they are included in the calculations which we present. Thus, the basic ring contains 32 arc dipoles and 52 quadrupoles, as well as sextupoles and octupoles for chromaticity and higher order corrections. Relevant to the present work, there are also 24 horizontal and 28 vertical dipole corrector magnets to be used for orbit correction and equal numbers of horizontal and

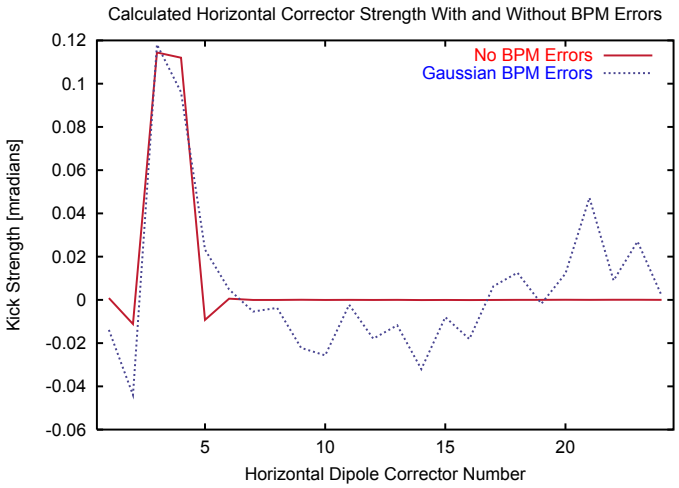

Figure 2. Three-bump correction scheme for 1mm horizontal offset of quadrupole Q07. Horizontal dipole corrector kick strengths are shown. Without errors in the BPM signals, only two correctors are activated, while BPM errors lead to further corrector activation.

A. Achromatic Arc of Four FODO Cells in Succession. Each FODO Cell Contains:	
Element	Length [meters]
Quadrupole Magnet	0.5
Drift Space	1.0
Sector Bending Magnet	1.5
Drift Space	1.0
Quadrupole Magnet	0.5
Drift Space	1.0
Sector Bending Magnet	1.5
Drift Space	1.0
B. Straight Section of Two Doublet Cells and Long Drift Spaces for Insertions:	
Element	Length [meters]
Quadrupole Magnet	0.5
Drift Space	6.85
Quadrupole Magnet	0.7
Drift Space	0.4
Quadrupole Magnet	0.55
Drift Space	12.5
Quadrupole Magnet	0.55
Drift Space	0.4
Quadrupole Magnet	0.7
Drift Space	6.85

TABLE 1. Basic SNS Ring Lattice Structure: Four Superperiods, Each Containing achromatic arcs and straight sections.

vertical beam position monitors to provide the orbit correction information. The lattice is tunable in the range $4 < \nu_{x,y} < 7$, and acceptable sets of lattice functions can be found between $5 < \nu_{x,y} < 7$. The present calculations are restricted to the baseline SNS operating point of $\nu_x = 6.23$, $\nu_y = 6.20$ and to natural chromaticity (all sextupoles turned off).

In this work we study the effects of closed orbit-deflecting errors in the 32 ring dipoles and 52 quadrupoles. This will be done using ORBIT [1], a comprehensive beam dynamics code for high intensity rings. A good description of ORBIT's scope and capabilities is given in Ref. [2]. In the present calculations, we use the complete model for the injection process and proton-foil interactions. We use a correlated transverse painting scheme that gives total (x+y) emittances of about 165π mm-mrad at the 10^{-3} level and total losses below 10^{-4} when errors are not present. The foil model includes multiple Coulomb scattering and slowing down, Rutherford scattering, and nuclear elastic and inelastic scattering with a carbon foil of assumed thickness 300 $\mu g/cm^2$. Particle tracking through the lattice is carried out with a symplectic tracking scheme including hard edge fringe fields. Collective effects are modeled using the 2.5D transverse space charge model, and longitudinal transport with space charge and the dominant extraction kicker impedance. Correct incorporation of transverse impedance effects requires the use of the 3D space charge routine, making the calculations very time consuming. Fortunately, a test calculation with these capabilities activated shows that, at full power of 1.44 MW, the beam is stable with respect to the dominant extraction kicker impedance. Therefore, it is not necessary to consider transverse impedances or 3D space charge modeling here. Losses are evaluated by the placement of apertures and collimators around the ring using ORBIT's aperture and collimation modules. For these studies, we set all apertures

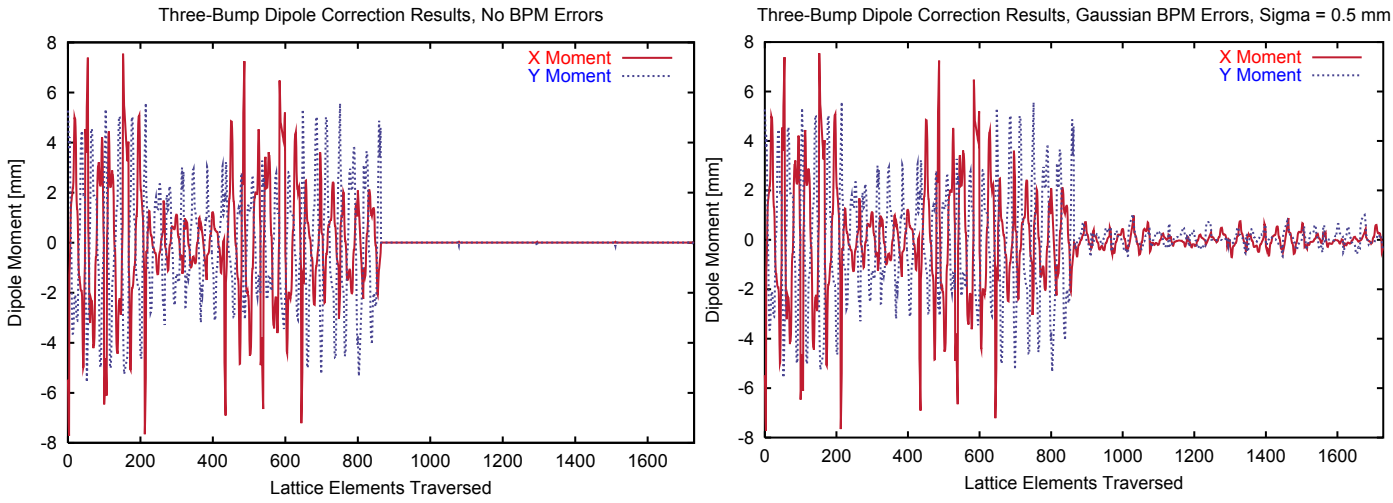

Figure 3. Three-bump correction scheme for 1mm offset of quadrupole Q52. Horizontal and Vertical dipole moments are shown for 8 turns. The first four turns are without correction, while the last four are with correction. The left hand plot was calculated assuming no errors in the BPM signals. The right hand plot assumes errors in the BPM signals, distributed randomly with a Gaussian distribution and sigma = 0.5 mm.

and collimators, except for the adjustable scrapers, to perfect absorbers. The adjustable scrapers are treated using the full collimation model, which contains the same physics as the foil model, except for the material and thickness: tantalum of thickness 4.5 mm backed by copper of thickness 14.55 mm.

A comprehensive selection of magnet alignment and field errors can be studied through ORBIT's error module. These can be specified for selected magnets or assigned by random distribution to groups of magnets. In this work we utilize both assignment schemes: direct assignment to individual magnets to ascertain the effects of specific errors or activation of individual dipole correctors to determine the orbit response matrix [3], and random distributions of errors to carry out realistic calculations of the effects of errors in the ring and of the usefulness of proposed correction schemes. The orbit correction model in ORBIT works by adjusting the dipole corrector magnet kick strengths to minimize, in a least squares sense, the sum of the squares of all the BPM signals for a chosen beam.

The module can carry this minimization out in either of two ways: 1) direct minimization using either the calculus-based VMCON [4] optimization package or the genetic algorithm optimization package GALIB [5], both of which are accessible to ORBIT through its driver shell, SuperCode [6]; or 2) minimization of the difference between the observed BPM signals and the product of the orbit response matrix with a vector consisting of the dipole corrector strengths to be determined. To use this latter method, it is first necessary to obtain the orbit response matrix. This is done by recording the BPM signals resulting from the activation of a standard (say one milliradian) kick in each dipole corrector node, in succession. Thus, from the standard activation of each of 52 dipole corrector nodes we obtain a vector, in a linear algebra sense, of 88 BPM signal values. We combine these vectors as columns to create an 88 × 52 matrix, R, the orbit response matrix of the SNS Ring. Under the assumption that the orbit deviations which give the BPM signals due either to separate magnet errors or to dipole corrector node kicks superpose linearly, then these signals may be minimized for any set of orbit-deflecting errors by setting the dipole corrector strengths to minimize the square of the vector $V = E - R \times D$, where E is the 88 dimensional vector of BPM signals due to the errors and D is the 52 dimensional vector of dipole corrector kick strengths. We note that the matrix R is not invertible and that the system is underdetermined, so that the best we can do is to minimize the vector V. In general, an exact solution is not possible. Most of the calculations presented in this paper were carried out using the direct minimization method with the VMCON optimizer. We are currently investigating the orbit response matrix method, and will report the results of this investigation in a later publication.

In the present calculations, we determine the corrector strengths using a pencil beam with initial coordinates on the desired (error free) closed orbit. Without magnet errors, this beam lies precisely on the closed orbit. By minimizing the excursions of this beam in the presence of errors we align the desired and actual closed orbits as much as possible. One additional feature of the orbit correction scheme is the option of statistically including the effects of errors in the BPM signals into the function to be optimized. We will show here that, with realistic values, such errors impact the desired correction scheme only slightly.

As stated above, we have developed a comprehensive set of computational models for magnet alignment and field errors. It is our intent to study all these errors and their correction for realistic tolerances in the SNS Ring. This paper constitutes the first such study, and we focus on three types of error that effect the closed orbit. In the following we present our analysis of quadrupole displacement errors in Sect. 2, dipole displacement and field errors in Sect. 3, and a summary of our results in Sect. 4. Other alignment errors, such as rotations leading to roll, pitch, and yaw, and errors involving sextupoles and octupoles will be examined in future studies. Because of the higher order of sextupole and octupole fields, alignment errors involving these magnets are expected to have small effects on the closed

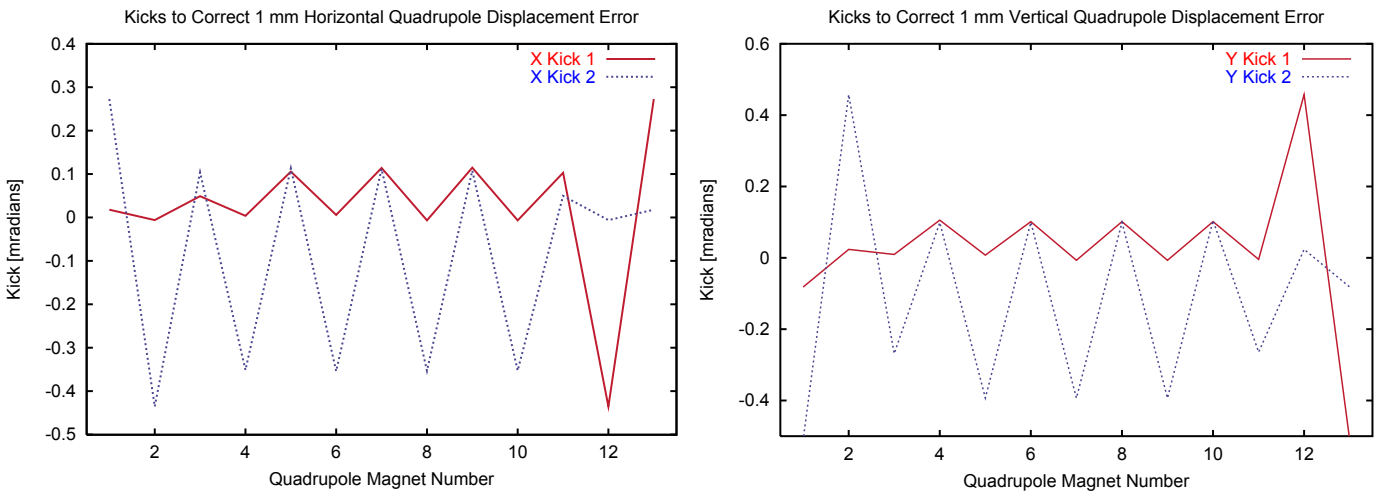

Figure 4. Horizontal and vertical kicker strengths needed to correct 1 mm horizontal and vertical offsets in the 13 quadrupoles of the first superperiod are shown in the left and right hand plots, respectively.

orbit, although the very presence of any sextupole or octupole fields does introduce coupling between the horizontal and vertical transverse motions.

QUADRUPOLE DISPLACEMENT ERRORS

The first topic we will treat in this paper is that of quadrupole displacement errors in the SNS ring. We define horizontal and vertical quadrupole displacement errors to be uniform displacements of the magnet in or out or up or down, respectively. There are 52 quadrupole magnets in the ring and, because of the fourfold ring symmetry, for determining corrector strengths it is only necessary to focus on the 13 magnets of one period. This is not true when losses are considered, because the apertures and collimators do not obey the fourfold symmetry. We begin by examining the pencil beam deviation caused by a 1 mm displacement in each individual quadrupole. Because the sextupole and skew quadrupole strengths are set to zero in this natural chromaticity case, the vertical and horizontal planes are decoupled to lowest order and the horizontal and vertical displacements lead to horizontal and vertical orbit deviations, respectively. Figure 1 shows the maximum horizontal and vertical orbit deviations of the pencil beam for 1 mm displacements of each of the 13 quadrupoles in the first superperiod. Focusing now on the curves for the uncorrected errors, we note that this plot repeats exactly for each of the three remaining superperiods. While the maximum vertical and most of the horizontal pencil beam orbit deviations vary in the range 2-5 mm, the maximum horizontal deviations for the displaced second and twelfth magnets peak above 9 mm. These magnets are focusing doublet quadrupoles in the straight sections, and their locations correspond to the maximum horizontal beta function values, namely $\beta_x = 27$ m. It is therefore not surprising that the horizontal uncorrected orbit attains its maxima at these locations.

Correction of these quadrupole displacement errors is achieved by adjusting the dipole kicker magnet strengths to minimize the orbit deviations of the pencil beam. In SNS the information about such deviations comes in the form of BPM signals from the 44 horizontal and 44 vertical beam position monitors. In the present ORBIT calculations, these BPMs are included in the lattice and their signals are obtained, with or

Magnet	Horizontal Corrector 1		Horizontal Corrector 2		Vertical Corrector 1		Vertical Corrector 2	
	Corrector #	Kick [mrad]	Corrector #	Kick [mrad]	Corrector #	Kick [mrad]	Corrector #	Kick [mrad]
Q01	DX24	0.0182	DX01	0.2729	DY28	-0.0821	DY01	-0.5102
Q02	DX24	-0.0057	DX01	-0.4351	DY28	0.0236	DY01	0.4576
Q03	DX01	0.0493	DX02	0.1042	DY02	0.0096	DY03	-0.2686
Q04	DX02	0.0041	DX03	-0.3510	DY02	0.1055	DY03	0.0989
Q05	DX02	0.1058	DX03	0.1137	DY03	0.0074	DY04	-0.3929
Q06	DX03	0.0061	DX04	-0.3537	DY03	0.1014	DY04	0.0994
Q07	DX03	0.1144	DX04	0.1120	DY03	-0.0068	DY04	-0.3933
Q08	DX03	-0.0063	DX04	-0.3526	DY04	0.1015	DY05	0.0991
Q09	DX04	0.1149	DX05	0.1082	DY04	-0.0068	DY05	-0.3933
Q10	DX04	-0.0064	DX05	-0.3524	DY05	0.1013	DY06	0.1048
Q11	DX05	0.1032	DX06	0.0502	DY05	-0.0045	DY06	-0.2645
Q12	DX06	-0.4351	DX07	-0.0057	DY07	0.4574	DY08	0.0237
Q13	DX06	0.2730	DX07	0.0182	DY07	-0.5102	DY08	-0.0821

TABLE 2. Dipole Corrector Selection and Kick Strengths Required to Correct 1 mm Horizontal and Vertical Displacement Errors of Specified Quadrupole Magnets

without errors, as center of charge beam positions in millimeters for the ring beam. Without errors, the BPM nodes return the exact dipole moments of any selected longitudinal portion of the beam in millimeters. When errors are invoked, a random component is added to each exact BPM signal. In the calculations here, when BPM errors are included, we assume a truncated Gaussian distribution with mean of 0 mm, sigma of 0.5 mm, and cutoff of ±1 mm.

In our ORBIT calculations, we adjust the strengths of the 24 horizontal and 28 vertical dipole corrector magnets, which are also included in the computational lattice. To do this, we use the optimization routine VMCON [4] to minimize the least square sum of the BPM signals, with or without errors, due to the pencil beam. The results of this correction for 1 mm displacements of the first 13 quadrupole magnets are shown in Figure 1, both with and without assumed BPM errors. We see that the maximum deviations of the pencil beam orbit are less than 2 mm in either case, so the dipole corrector magnets successfully correct individual quadrupole displacement errors.

In performing the minimization of the BPM signals without BPM errors for displacement errors of each individual quadrupole magnet, we find that only two dipole corrector kicks are required for each error. The optimization routine chooses a three-bump orbit correction scheme [3], with the bumps corresponding to the quadrupole displacement error and to kicks from the two adjacent dipole correctors. Figure 2 shows the kick strengths in milliradians required to correct a 1 mm horizontal displacement of Q07, the seventh quadrupole in the ring, taken from the injection point. We see that only two correctors, those surrounding Q07, are significantly activated when the BPM signal contains no error. The resulting kick strengths are also shown with random BPM errors assumed, and although the largest kicks are almost unchanged, all the kickers are activated to some extent to correct the erroneous signals due to the BPM errors.

The BPM signals obtained during the correction of Q52 are shown in Figure 3, both without and with BPM errors. The plots show the signal taken over 8 turns, the first 4 turns without correction and the last 4 turns following correction. Without BPM errors, the dipole moment is essentially zero except for tiny perturbations at the quadrupole. When errors in the BPM signals are included, the maximum position errors remain small, but the corrected orbit is noisy and not localized in the ring.

The required dipole corrector magnets and their associated kick strengths to correct 1 mm displacement errors are shown for the first superperiod in Table 2 and plotted in Figure 4. The strengths are again the same for each superperiod. Using these strengths, we can define an orbit correction matrix C_{ij} = the kick in milliradians required from the i^{th} dipole corrector magnet to correct a 1 mm displacement of the j^{th} magnet. To the extent that the effects of the quadrupole displacements superpose linearly in the beam position signals, the matrix C can be multiplied by an actual set of magnet displacements to correct the combined effects on the orbit. We have compared the corrector strengths calculated this way to those obtained

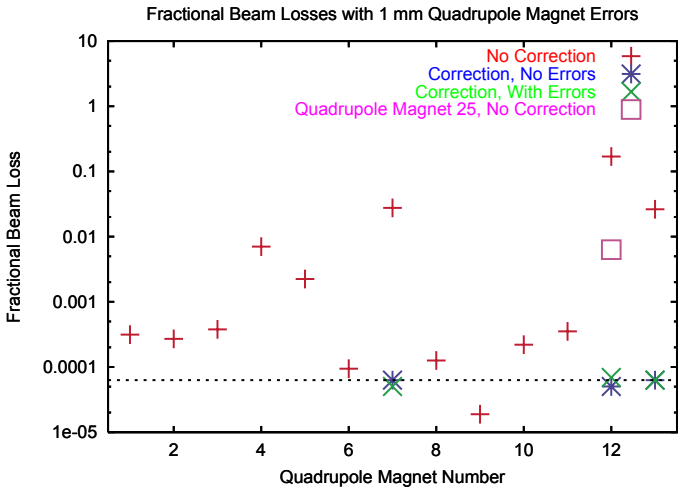

Figure 5. Fractional beam losses with 1 mm horizontal and 1 mm vertical displacements of selected quadrupoles. The horizontal line shows fractional beam loss with no magnet errors.

from direct optimization for randomly generated sets of magnet errors, and the results are in excellent agreement. This demonstration of linearity suggests that the orbit response matrix method for orbit correction will work well, at least for quadrupole displacement errors. However, it should be mentioned that unlike the orbit response matrix R, which relates BPM signals to dipole kick strengths that are known in general, the orbit correction matrix C can not be used in practical situations because the sizes of the magnet errors are not known.

We now consider the beam losses induced by 1 mm horizontal and 1 mm vertical displacement of selected quadrupole magnets in a standard SNS beam accumulation. The accumulation was carried out as described in the introduction to this paper. Specifically, correlated injection painting was applied to accumulate a beam of 1.5×10^{14} 1 GeV protons over 1060 turns, which corresponds to 1.44 MW operation at a pulse rate of 60 Hz. Figure 5 shows the results of these calculations. The horizontal line gives the fractional beam loss, less than 1×10^{-4}, when no magnets are displaced. The red symbols show

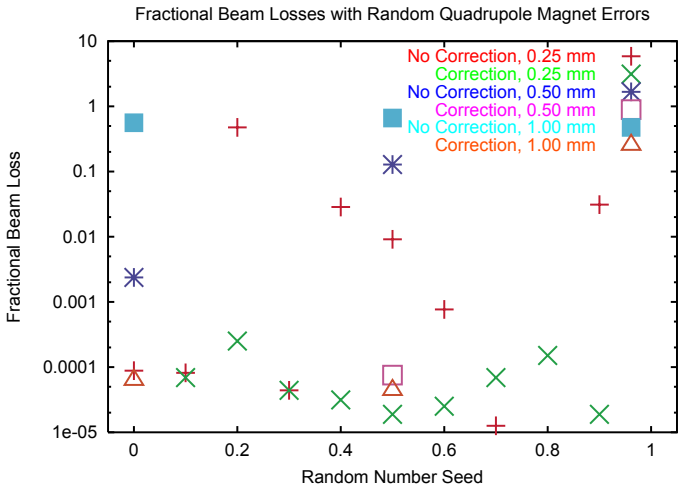

Figure 6. Fractional beam losses with randomly distributed horizontal and vertical displacements all quadrupoles.

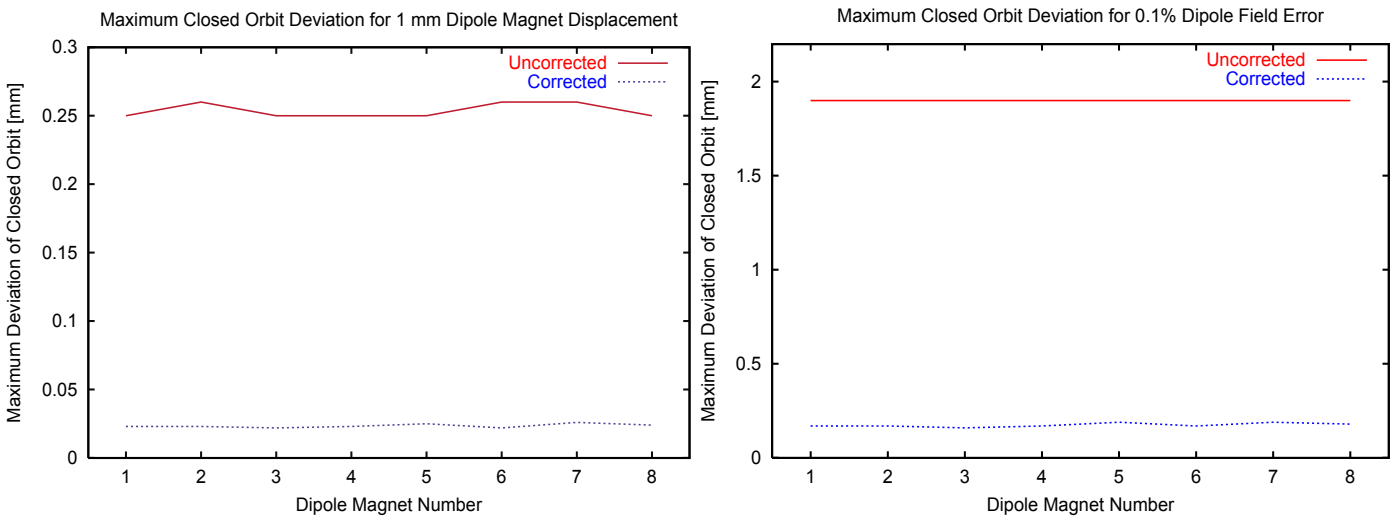

Figure 7. Uncorrected and corr
dipole magnet field errors (right hand plot) for dipoles in the first superperiod.

the losses for the displacement of each of the 13 individual quadrupoles in the first superperiod. These vary from less than 1×10^{-4} to more than 15% in the case of Q12. Unlike the orbit deviations and correction strengths, the losses do not obey the fourfold ring symmetry. The constraining apertures in the ring are the collimators in the second straight section, especially the adjustable scrapers that serve as the first point of contact for beam destined to be lost. Because of this, magnet displacements in the first superperiod tend to lead to greater losses than displacements in other superperiods. An example is shown in Figure 5, where the loss resulting from displacement of Q25, exactly one superperiod downstream from Q12 and thus after the collimation, is seen to be one and one half orders of magnitude less than that resulting from displacement of Q12. Correction of the magnet errors is seen to cure the losses from individual magnet displacements. Losses with correction were calculated only for the 7th, 12th, and 13th quadrupoles, and these were all at or below the 10^{-4} level. It is interesting that BPM errors have little effect on the observed losses for these cases. The plausibility of this can be inferred by looking at the results in Figs. 3 and 4, which show that the effect of BPM errors is to add a small jitter to the results without errors, but not to change the overall picture significantly.

In order to consider a somewhat more realistic set of cases, a study was carried out in which horizontal and vertical displacements were assigned at random to all 52 ring quadrupoles. For this assignment, a uniform distribution satisfying $-a$ < displacement error < a was used. In most cases, a was taken to be 0.25 mm, consistent with the SNS displacement requirements; but some cases were also run with a = 0.50 mm and a = 1.00 mm. In all cases, full SNS beam accumulation calculations were performed and losses tabulated, using the same dynamic assumptions as in the single quadrupole displacement loss calculations. For the default case of a = 0.25 mm,

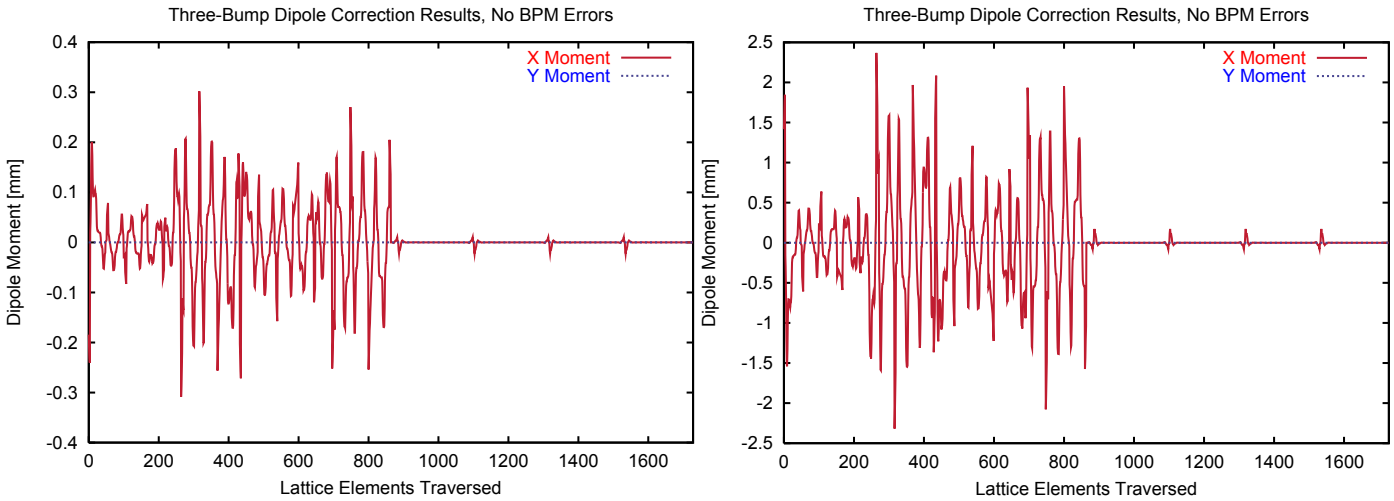

Figure 8. Three-bump correction scheme for 1mm offset (left hand plot) and 0.1% field error (right hand side) of dipole 04. Horizontal dipole moments are shown for 8 turns. The first 4 turns are without correction, while the last 4 turns are with correction. The plots were calculated assuming no errors in the BPM signals.

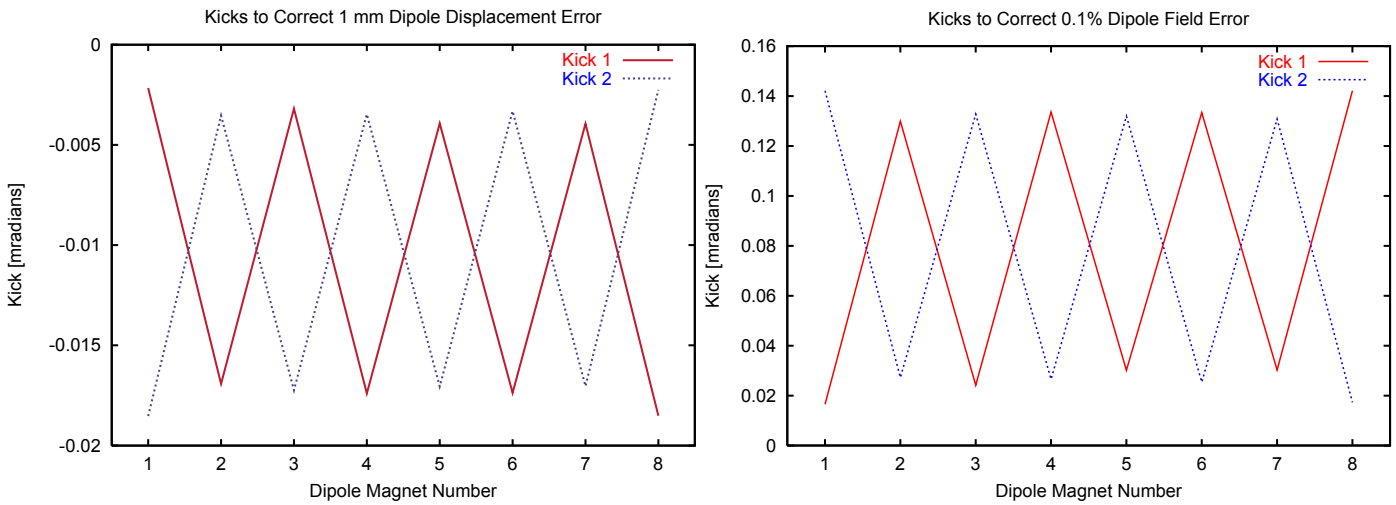

Figure 9. Horizontal kicker strengths needed to correct 1 mm horizontal offsets (left hand plot) and 0.1% dipole field errors (right hand plot) in the first superperiod of the ring.

the calculation was performed 10 times with different random number seeds ranging from 0 → 0.9 in intervals of 0.1. The results, plotted in red in Figure 6, show a variation from less than 10^{-5} (seed = 0.8) to 48% of the beam (seed = 0.2). For the worst case uncorrected lattice, the moments of the pencil beam showed maximum values of 13 mm (horizontal) and 12 mm (vertical). The variation in loss values is not surprising in light of the results for the individual quadrupole displacements: some magnet displacements lead to little loss while others can have a major impact. Depending on the particular random displacements corresponding to various seeds, losses can be small or large.

A more important question regards the beam losses when the dipole corrector magnets are activated. For each of the seed values, a correction calculation was carried out. The corrector strengths were calculated in two ways: first by direct least square minimization of the BPM signals for the standard pencil beam with initial coordinates on the desired closed orbit, and second by matrix multiplication of the orbit correction matrix C defined above with the displacements of the quadrupoles obtained from the random distribution with the given seed. The resulting dipole corrector strengths proved to be in excellent agreement for the two methods, indicating that the effects of the displacement errors in this size range superpose linearly. The resulting losses for $a = 0.25$ mm, plotted in green in Figure 6, are less than 10^{-4} in all but two cases, with a worst-case value of 2.5×10^{-4} when the seed is 0.2. In this case of corrected lattice errors, the maximum values of the moments of the pencil beam are still less than 2 mm. These results are clearly quite satisfactory, demonstrating that the anticipated errors can be corrected to limit total losses well below the required 10^{-3} for a variety of cases. These calculations were carried out assuming no errors in the BPM signals but, as we shall show later, the results with BPM errors assumed are also acceptable. For two of the seed values, namely 0 and 0.5, the calculations were repeated for larger displacement ranges $a = 0.5$ mm and $a = 1.00$ mm. In both these cases, with $a = 1.00$ mm, the losses exceeded 50% of the beam, but with correction they dropped to less than 10^{-4}, as shown in Figure 6.

We therefore conclude that losses caused by orbit deviations due to quadrupole displacement errors are readily correctable in the SNS ring.

DIPOLE DISPLACEMENT AND FIELD ERRORS

Let us now consider the effects of dipole displacement and field errors. We define horizontal dipole displacement errors to be uniform displacements of the magnet in or out along its center line and vertical dipole displacement errors to be uniform displacements of the magnet up or down. By field errors, we simply mean changes in the dipole bending field strength. With the symplectic transport models and hard edge fringe fields used here, vertical dipole displacements have no effect on the beam nor do any of these errors effect the vertical motion, so we report the pencil beam results only for horizontal motion with horizontal dipole displacement errors and with field errors. The simulations are all performed in the full six dimensional phase space.

As with quadrupole displacement errors, we begin our study of dipole errors by considering the effects of perturbing individual magnets. Figure 7 shows the maximum deviations of the pencil beam orbit for 1 mm displacements of the 8 first superperiod individual ring dipoles in the left hand plot and for 0.1% field errors of the same dipoles in the right hand plot, both without correction and with correction assuming no BPM errors. The simulations lead to the following conclusions: 1) the maximum orbit deviations not only demonstrate the fourfold SNS ring periodicity, but are nearly independent of which dipole is perturbed; 2) even without correction the dipole displacement and field errors are small, disturbing the orbit by about 0.25 mm in the former case and by less than 2 mm in the latter; and 3) with correction the orbit deviations are much smaller yet, being < 0.2 mm in all cases.

As with the quadrupole displacement errors, the correction of individual dipole errors localizes the maximum orbit

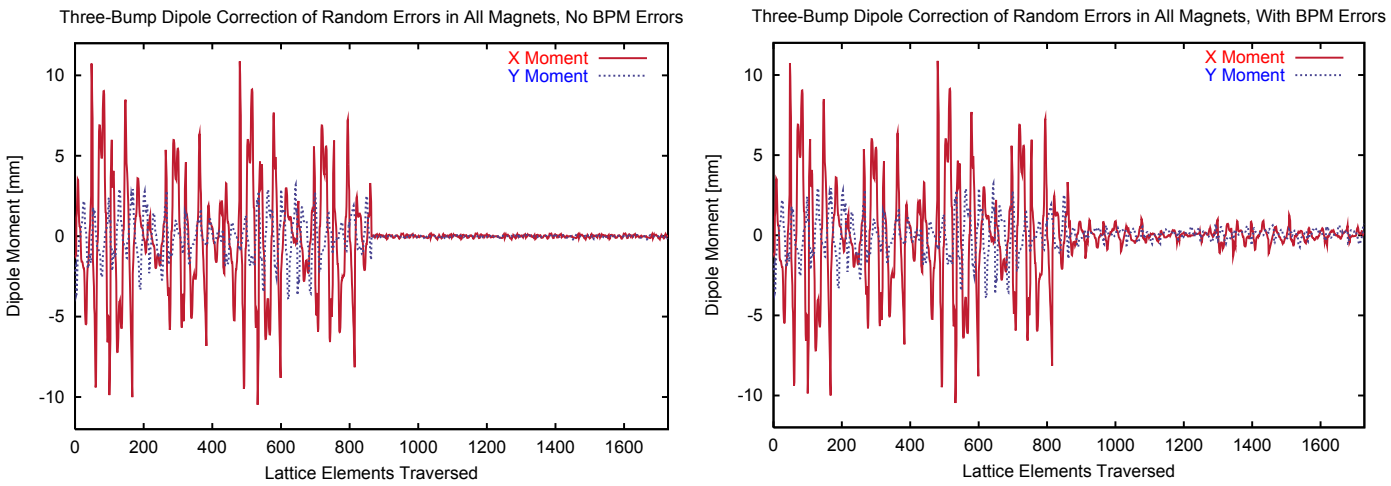

Figure 10. Three-bump correction scheme for random quadrupole displacement, dipole displacement, and dipole field errors. Horizontal and vertical dipole moments are shown for 8 turns. The first four turns are without correction, while the last four turns are with correction. The left hand plot was calculated assuming no errors in the BPM signals, while the right hand plot was calculated with BPM errors.

deviation to the vicinity of the magnet having the error. Figure 8 shows the BPM signals for eight turns, the first four turns without correction and the second four turns following correction, for a 1 mm displacement of dipole number 4 in the left hand plot and for a 0.1% field error in dipole number 4 in the right hand plot. The correction was performed using a pencil beam with initial coordinates on the desired closed orbit. For both types of error, the corrected BPM signal shows only tiny orbit deviations in the immediate vicinity of the dipole with error. These results were all obtained under the assumption of no BPM errors.

An examination of the dipole corrector kick strengths obtained in the correction process shows that once again the optimization scheme selects the three-bump method. For each individual magnet error, the correction scheme selects the adjacent dipole corrector nodes to minimize the BPM signals. Outside the region determined by the two activated correctors and the magnet with error, the signals are essentially zero. The two dipole corrector kick strengths needed to correct 1 mm displacement and 0.1% field errors are plotted versus ring dipole number in Figure 9. As with the orbit deviations, the required kick strengths satisfy the fourfold symmetry of the SNS ring lattice. Comparison with Figure 4 shows that the kick strengths required to correct 1 mm quadrupole displacement errors are about twice the size of those required to correct 0.1% dipole field errors, and about twenty times larger than those required to correct 1 mm dipole displacement errors.

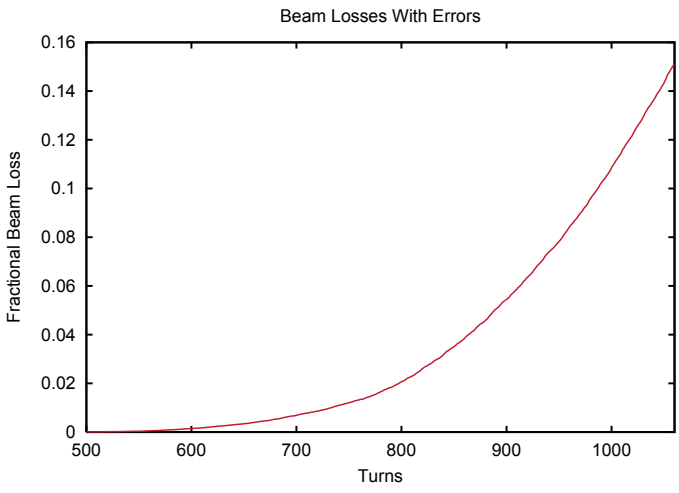

Figure 11. Fractional beam loss versus time (turn number) for full beam accumulation with no error correction at 1.44 MW.

Calculations for more realistic situations were carried out with randomly assigned sets of dipole errors. As with the random quadrupole errors, the dipole errors were assigned from uniform random distributions with $-a <$ error $< a$. For dipole displacement errors, a was chosen to be 0.25 mm in keeping with the SNS specifications and errors assigned for the 10 random number seeds $0 \rightarrow 0.9$ in intervals of 0.1. Closed orbit calculations showed a worst-case maximum closed orbit deviation of 0.9 mm. A complete beam accumulation calculation was carried out without correction for this case and losses were below the 10^{-4} level. The same exercise was performed for random dipole field errors with a chosen to be 0.1%, again in accord with SNS specifications. In these calculations, the worst-case losses were all below the 10^{-4} level. The maximum deviations occur in the arcs, rather than in the collimation section, where the limiting apertures are found.

SUMMARY AND CONCLUSIONS

As a summary of this work we present the following case: we consider a lattice with simultaneous random quadrupole displacement errors, random dipole displacement errors, and random dipole field errors. All three sets of errors are assigned from uniform distributions with $a = 0.25$ mm, $a = 0.25$ mm, and $a = 0.1\%$, respectively, in accord with SNS specifications. The calculations were performed for a number of different seed values, and we present the worst-case results here.

Figure 10 shows the horizontal and vertical moments of the standard pencil beam taken over eight turns. The left hand

plot was calculated without BPM errors, and the right hand plot includes BPM errors. In the first four turns the magnet errors are uncorrected and the vertical and horizontal moments are seen to peak at values of 11 mm; while in the last four turns the corrected moments are much less than 1 mm without BPM errors and never exceed about 1 mm, even with BPM errors. The inclusion of BPM errors adds a little noise to the corrected moments but the overall effect is minor.

Figure 11 shows the fractional beam loss versus turn number for the full beam accumulation without error correction at 1.44 MW. Without any error correction, the fractional beam loss of this worst case exceeds 15%. In contrast, with correction fractional losses are less than 10^{-4} whether BPM errors are assumed or not. We find this result for many cases, namely, that BPM signal errors at the anticipated level do not seriously affect the correction scheme.

A final comment is in order regarding the adequacy of the dipole corrector strengths required for correction. In all cases examined here, the maximum required kick strengths were less than 0.3 milliradians change in the orbit angle. Because the dipole correctors are capable of kicks in excess of 0.5 milliradians, the corrections are well within the capabilities of the system. Thus, the proposed SNS orbit correction system, consisting of 88 BPMs and 52 dipole corrector magnets, is sufficient to correct the closed orbit-deflecting magnet errors studied here to the required level.

In summary, we have considered the effect and correction of three types of orbit-deflecting errors in SNS: quadrupole displacement errors, dipole displacement errors, and dipole field errors. Of these, the quadrupole displacement errors show the greatest severity at the anticipated level, followed by dipole field errors and finally by dipole displacement errors, both with respect to orbit deflections and to beam losses. The dipole field and displacement errors lead to small orbit deflections and also fail to induce significant losses. We study the correction of these orbit-deflecting errors using the proposed system of 88 ring BPMs and 52 dipole corrector magnets. Correction is carried out numerically in the ORBIT code using VMCON to adjust the kick strengths of the dipole corrector magnets to minimize the sum of the squares of the BPM signals. In future work we will present this minimization using an orbit response matrix technique. For all three types of error and perturbations of individual magnets, the correction algorithm always chooses the three-bump method to localize the orbit displacement to the region between the magnet and its adjacent correctors and to reduce the maximum orbit deflection. If we also consider the effect of errors in the BPM signals, we find that the three-bump scheme becomes imperfect, with some activation of nonadjacent corrector magnets and some noise in the orbit deflection signal outside the three-bump vicinity. At the anticipated BPM uncertainty level these effects are small. The dipole corrector kick strengths obtained from correction of known errors can be used to set up a matrix which can be multiplied by arbitrary sets of magnet errors to obtain sets of kicks that agree closely with those obtained directly from the optimizer for those errors. When high intensity calculations are carried out to study beam losses, it is seen that the SNS orbit correction system, even with BPM uncertainties, is sufficient to correct losses to less than 10^{-4} in nearly all cases, even those for which uncorrected losses constitute a large portion of the beam.

ACKNOWLEDGEMENTS

I wish to thank Stuart Henderson and Sarah Cousineau for useful discussions and suggestions during this investigation. I also wish to thank my mentor Jeff Holmes for his guidance and knowledge.

* Research on the Spallation Neutron Source is sponsored by the Division of Materials Science, U.S. Department of Energy, under contract number DE-AC05-96OR22464 with UT-Battelle Corporation for Oak Ridge National Laboratory.

REFERENCES

[1] J. Galambos, J. Holmes, D. Olsen, A., http://www.sns.gov//APGroup/Codes/Codes.html.

[2] J. Holmes, S. Cousineau, V. Danilov, S. Henderson, A. Shishlo, Y. Sato, W. Chou, L. Michelotti, and F. Ostiguy, ICFA Beam Dynamics Newsletter 30, (April, 2003) 100.

[3] S. Y. Lee, *Accelerator Physics*, World Scientific Publishing Company, (Singapore, 1999), see page 111.

[4] R. L. Crane, K. E. Hillstrom, and M. Minkoff, “Solution of the General Nonlinear Programming Problem with Subroutine VMCON”, ANL-80-64, (Argonne National Laboratory, July, 1980).

[5] GAlib, A C++ Library of Genetic Algorithm Components, http://lancet.mit.edu/ga/.

[6] S. W. Haney, “Using and Programming the SuperCode”, UCRL-ID-118982, (Lawrence Livermore Laboratory, Oct. 24, 1994).